

inverter based on two AlGaIn-GaN HFETs with threshold voltages of -0.5V (T1) and -1.0V (T2). The epilayer design of the T2 HFET was similar to that of T1. However, to increase the threshold voltage of transistor T2, the AlGaIn barrier thickness was increased to 20nm . The inverter also used a GaN Schottky barrier diode connected in series with the HFET gate for level shifting. At room temperature, the measured inverter characteristics exhibited a large gain (up to 180) and had a noise margin of $\sim 0.5\text{V}$. We also tested the performance of the inverter (without the Schottky diode) at elevated temperatures (see Fig. 3). The estimated temperature coefficient of the switching voltage of the device was $\sim 3.5\text{mV}/^\circ\text{C}$ up to 90°C , which is about three times higher than in a similar silicon device [5].

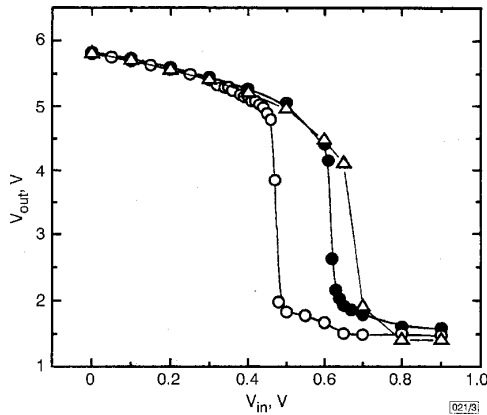


Fig. 3 Characteristics of inverter

Based on two AlGaIn-GaN HFETs and without level lifting Schottky diode at three different temperatures
Estimated voltage switching coefficient is $3.5\text{mV}/^\circ\text{C}$
 $\circ T = 17.5^\circ\text{C}$
 $\bullet T = 50^\circ\text{C}$
 $\triangle T = 75^\circ\text{C}$

The measured device characteristics and the inverter transfer curves are in good agreement with the simulated dependencies that were obtained using the AIM-SPICE AlGaIn-GaN HFET model [6]. Using the calculated temperature coefficients of the electron mobility at elevated temperatures and the previously measured temperature coefficient of the threshold voltage, we predict that such an inverter should operate up to $\sim 230^\circ\text{C}$. A much higher operating temperature and a larger noise margin can be obtained using a switching transistor with a more positive threshold voltage and with an optimised transistor load. Both the measured data and simulated results clearly demonstrate that GaN-based digital circuits are possible.

In conclusion, we have fabricated a low-threshold voltage AlGaIn-GaN HFET and demonstrated the first GaN-based digital circuit. The HFET devices with ultra-thin $\text{Al}_{0.25}\text{Ga}_{0.75}\text{N}$ barrier demonstrated very low leakage currents and high electric breakdown fields. The AlGaIn-GaN HFET-based inverter exhibited a positive switching voltage coefficient of $3.5\text{mV}/\text{K}$ and had a stable performance at elevated temperatures up to 90°C . The experimental data and simulation results indicate that further improvement in the device characteristics could make GaN-based devices suitable for high temperature digital applications.

Acknowledgment: The work has been supported by the Office of Naval Research under contract No. N00014-97-C-0033 (Project Monitors C. Wood and J. Zolper).

© IEE 1998

1 October 1998

Electronics Letters Online No: 19981665

R. Gaska (APA Optica, Inc., 2950 NE 84th Lane, Blaine, MN 55449, USA)

J. Deng and M.S. Shur (CIEEM and Department of ECSE, Rensselaer Polytechnic Institute, CII 9015, 110 8th Street, Troy, NY 12180-3590, USA)

2368

References

- GASKA, R., BYKHOVSKI, A.D., SHUR, M.S., YANG, J., and OSINSKY, A.: 'Piezoeffect and gate current in AlGaIn/GaN high electron mobility transistors', *Appl. Phys. Lett.*, 1997, **71**, pp. 3673-3675
- ASIF KHAN, M., CHEN, Q., SUN, C.J., YANG, J.W., BLASINGAME, M., SHUR, M.S., and PARK, H.: 'Enhancement and depletion mode GaN/AlGaIn heterostructure field effect transistors', *Appl. Phys. Lett.*, 1996, **68**, (4) pp. 514-516
- GASKA, R., CHEN, Q., ASIF KHAN, M., PING, A., ADESIDA, I., and SHUR, M.S.: 'AlGaIn-GaN heterostructure FETs with offset gate design', *Electron. Lett.*, 1997, **33**, (14) pp. 1255-1257
- WU, Y.-F., KELLER, B.P., KELLER, S., KAPOLNEK, D., KOZODOY, P., DENBAARS, S.P., and MISHRA, U.K.: 'Very high breakdown voltage and large transconductance realized on GaN heterojunction field effect transistors', *Appl. Phys. Lett.*, 1996, **69**, (10) pp. 1438-1440
- BROWN, R.B., and WU, K.: 'High temperature operation of silicon MOSFETs' in WILLANDER, M., and HARTNAGEL, H.L. (Eds.): 'High temperature electronics' (Chapman and Hall, 1996), p. 67
- FJELDLY, T., YTTERDAL, T., and SHUR, M.S.: 'Introduction to device and circuit modeling for VLSI' (John Wiley and Sons, New York, 1998)

Wideband CMOS current conveyor

A.M. Ismail and A.M. Soliman

A CMOS second generation current conveyor consisting of two matched differential pairs and based on the first generation current conveyor is presented. PSPICE simulations have shown that its performance is quite satisfactory for wideband current-mode signal processing.

Introduction: The second-generation current conveyor (CCII) is the most versatile building block in current mode signal processing [1]. To exploit wideband and wide dynamic range capabilities under low power operation of current-mode signal processing, a CCII based on the translinear loop has been proposed [2-4]. These translinear CMOS circuits exhibit an excellent current following behaviour from port X to port Z over a wide bandwidth but the voltage following property from port Y to port X is poor and the offset voltage is rather high. Other simple CMOS realisations of the CCII have been introduced [5-12]. In this Letter, a novel CMOS realisation of the CCII based on the long tail differential pair is introduced.

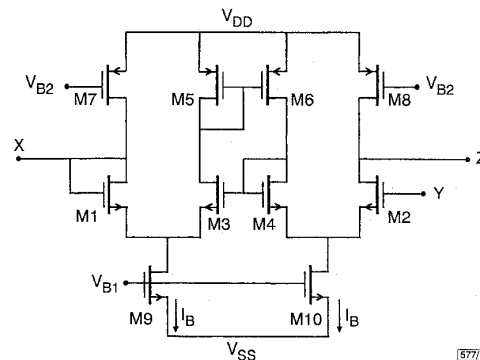


Fig. 1 Circuit configuration of proposed CCII

Circuit description: The circuit configuration of the proposed CCII is shown in Fig. 1. It consists mainly of two differential pairs (M1-M3 and M2-M4). It can be easily noted that transistors M3-M6 form the first generation current conveyor introduced in [1]. The action of the proposed CCII can be described as follows: Assuming that the two differential pairs M1, M3 and M2, M4 are perfectly matched, the CCI formed by M3-M6 conveys the voltage from the source of transistor M4 to the source of transistor M3 and the current from transistor M5 to transistor M6, thus the voltage v_Y applied to the gate of M2 does not affect the current flowing in M4 since the latter follows the current flowing in M3,

and, since the sources of transistors M1 and M2 have the same voltage (due to the action of the CCI) and carry the same current (since the currents in M3 and M4 are equal), the voltage v_y is conveyed to node X successfully. The current coming from X can be reproduced in Z without the need for current mirrors as shown in Fig. 1.

The voltage transfer function is given by

$$\frac{v_x}{v_y} = \frac{1}{1 + \frac{1}{g_m^2 r_o R_L}} \quad (1)$$

where g_m and r_o are the transconductance of the differential pair and the resistance seen at the drain of transistor M4 (before connecting it to its gate terminal), respectively. R_L is the load resistance connected at node X (R_L is replaced by R_X when no load is connected to the node X).

The resistance R_X at node X is given by

$$R_X = \frac{r_o}{1 + g_m^2 r_o^2} \quad (2)$$

With the simple configuration shown in Fig. 1, it follows therefore that R_X is very small and v_x follows exactly v_y .

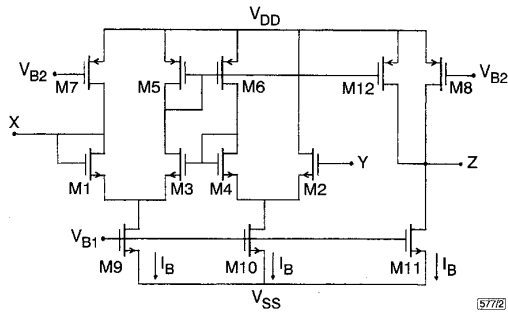


Fig. 2 Modified circuit configuration of CCII

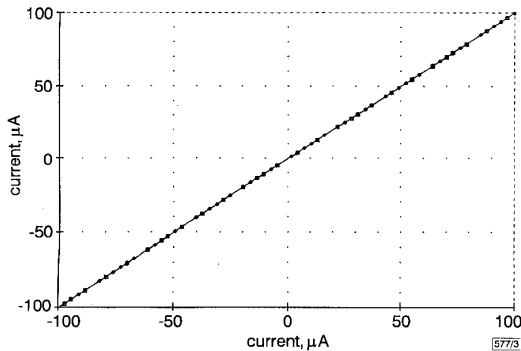


Fig. 3 Current transfer characteristics from node X to node Z

□ -I (V3)
◇ I (I5)

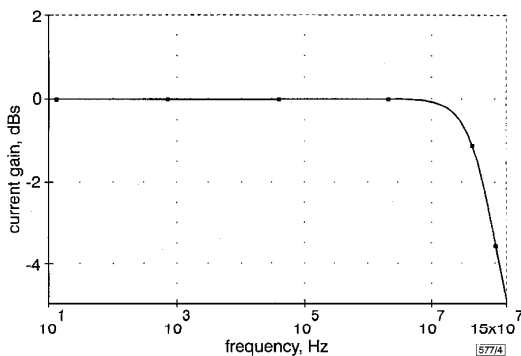


Fig. 4 Current gain in decibels of CCII circuit against frequency

It is noted that in the configuration of Fig. 1, the value of the voltage v_z at the node Z is restricted to be higher than ($v_y +$

$v_{DS2,max}$) for proper operation. To overcome this problem, the circuit is modified as shown in Fig. 2. The voltage v_z can then take values less than v_y which is necessary to design voltage amplifiers with gain less than unity.

The above analysis of the circuit operation confirms that the circuits shown in Figs. 1 and 2 are each CCII+ and their input-output relation can be described in terms of the ideal 3×3 matrix representation [1]. A CCII version can be easily realised by inverting the direction of i_z using current mirrors.

Table 1: W/L of transistors of CCII shown in Fig. 2

Transistor	Aspect ratio
M1-M4	35/1.4
M5, M6, M12	49/3.5
M7, M8	49/3.5
M9, M10, M11	35/2.8

PSPICE simulations: Performances of the CCII shown in Fig. 2 are simulated using PSPICE. Transistor aspect ratios in Table 1 and $0.7\mu\text{m}$ CMOS process are used. Supply voltages are $V_{DD} = -V_{SS} = 2.5\text{V}$ and I_B is set to $100\mu\text{A}$.

It is found that the resistance R_X is 8Ω . The offset voltage at node X when Y is grounded is $< 0.5\text{mV}$. Fig. 3 shows the current transfer characteristics from node X to node Z. An excellent current-following action can be seen over the wide current range. Fig. 4 illustrates the current gain of the circuit against frequency. The simulations show that the circuit is also an excellent current follower that can be widely used in current-mode signal processing.

© IEE 1998

3 November 1998

Electronics Letters Online No: 19981680

A.M. Ismail and A.M. Soliman (Electronics and Communications Engineering Department, Cairo University, Giza, Egypt)

References

- 1 SEDRA, A.S., ROBERTS, G.W., and GOHN, F.: 'The current conveyor: history, progress and new results', *IEE Proc. G*, 1990, **137**, pp. 78-87
- 2 BRUNN, E.: 'CMOS High speed, high precision current conveyor and current feedback amplifier structures', *Int. J. Electron.*, 1993, **74**, pp. 93-100
- 3 FABRE, A.: 'Wideband translinear current conveyor', *Electron. Lett.*, 1984, **20**, pp. 241-242
- 4 ZELE, R.H., ALLSTOT, D.J., and FIEZ, T.S.F.: 'Fully balanced CMOS current-mode circuits', *IEEE J. Solid-State Circuits*, 1993, **28**, pp. 569-574
- 5 ELWAN, H.O., and SOLIMAN, A.M.: 'Novel CMOS differential voltage current conveyor and its applications', *IEE Proc. Circuits Devices Syst.*, 1997, **144**, pp. 195-200
- 6 ELWAN, H.O., and SOLIMAN, A.M.: 'A novel CMOS Current conveyor realization with an electronically tunable current mode ifiter suitable for VLSI', *IEEE Trans. Circuits Syst. II*, 1996, **43**, pp. 663-670
- 7 CHENG, M.C.H., and TOUMAZOU, C.: '3V CMOS current conveyor cell for VLSI technology', *Electron. Lett.*, 1993, **29**, pp. 317-318
- 8 CHA, H.-W., and WATANABE, K.: 'Wideband CMOS current conveyor', *Electron. Lett.*, 1996, **32**, pp. 1245-1246
- 9 OLIAEI, O., and PORTE, J.: 'Compound current conveyor (CCII+ and CCII)', *Electron. Lett.*, 1997, **33**, pp. 253-254
- 10 ELWAN, H.O., and SOLIMAN, A.M.: 'Low-voltage low-power CMOS current conveyors', *IEEE Trans. Circuits Syst. I*, 1997, **44**, pp. 828-835
- 11 LIU, S.I., TSAO, H.W., and WU, J.: 'CCII based continuous time filters with reduced gain bandwidth sensitivity', *IEE Proc. G*, 1991, **138**, pp. 210-216
- 12 SURAKAMPONTORN, W., RIEWRUJA, V., KUMWACHARA, K., and DEJHAN, K.: 'Accurate CMOS-based current conveyors', *IEEE Trans.*, 1991, **IM-40**, pp. 699-702